

## Nanostructured Composite Films for Dye-Sensitized Solar Cells by Electrostatic Layer-by-Layer Deposition

Alexander G. Agrios,<sup>\*,†</sup> Ilkay Cesar, Pascal Comte, M. K. Nazeeruddin, and Michael Grätzel

*Institut des Sciences et Ingénierie Chimiques,  
Ecole Polytechnique Fédérale de Lausanne,  
CH-1015 Lausanne, Switzerland*

Received July 19, 2006

Electrostatic layer-by-layer (ELBL) deposition is a simple procedure for constructing films by alternating layers of opposite charge.<sup>1</sup> It has been used to make thin, ordered polymer films<sup>2–6</sup> that can serve as templates for inorganic films<sup>7</sup> or nanoparticle growth.<sup>8–12</sup> ELBL techniques can also directly yield films of semiconductor nanoparticles.<sup>13,14</sup> TiO<sub>2</sub> nanoparticulate films, for example, can be fabricated by dipping a glass slide in a cationic polymer solution and then in a suspension of anionic TiO<sub>2</sub> particles, with intermediate rinsing and drying steps, and repeating until the desired film thickness is achieved. Alternately, an anionic polymer can be used along with cationic TiO<sub>2</sub> particles. All solutions and suspensions are aqueous, and the charge of the TiO<sub>2</sub> is controlled by pH.

ELBL semiconductor films have been used to make metal–metal oxide diodes as thin films<sup>15,16</sup> or as rectifiers in nanowires,<sup>17,18</sup> CdSe/polymer LEDs,<sup>19</sup> Au nanorod films for surface-enhanced Raman spectroscopy,<sup>20</sup> and photocata-

lytic films,<sup>21</sup> and to coat organic nanofibers with TiO<sub>2</sub>.<sup>22</sup> Aspects of the electrochemical behavior of ELBL TiO<sub>2</sub>/polymer films have been studied.<sup>23,24</sup> TiO<sub>2</sub> films made by ELBL were used in dye-sensitized solar cells<sup>25</sup> (DSCs) for the first time by He et al.,<sup>26</sup> who demonstrated that precise control of film thickness was possible by choosing the number of dipping cycles and that the resulting solar cells can have good efficiencies if made sufficiently thick. They also found empirically that using a cationic polymer and anionic TiO<sub>2</sub> resulted in better films than the converse. Each of their films was of uniform composition throughout its thickness.

In the present paper, we demonstrate some of the possibilities for making nanocomposite semiconductor films for DSCs using the ELBL method. Different materials can be used for different layers, and because each layer is quite thin (roughly a monolayer), ELBL deposition is a powerful tool for creating films that are highly structured in the *z*-direction. Here, we present films that incorporate large scattering particles or TiO<sub>2</sub> nanorods into nanospherical TiO<sub>2</sub> films for DSCs.

F-doped SnO<sub>2</sub>-coated glass (TEC-15, Hartford Glass Co., USA, 15 Ω/□) slides were coated by dipping them into beakers containing 100 mL of 1 g/L polymer solution (polydiallyldimethyl ammonium chloride (PDAC), 70 kDa, Aldrich), 2 g/L colloidal TiO<sub>2</sub> (16 nm nanoparticles made as previously described<sup>27</sup> but washed with pure water instead of ethanol), or 600 mL water (> 18 MΩ cm, Milli-Q), using the same dipping sequence and times as in ref 26 and automated using a modified fraction collector (Pharmacia LKB SuperFrac). All beakers contained 5 mM triethylamine, which keeps the pH near 11. A single beaker served as the second rinse following both the polymer and TiO<sub>2</sub> steps.

Coated slides were cut in half vertically, giving two strips that could then be subject to different treatments for comparison; for example, sintered vs unsintered, or transparent + scattering layers vs transparent layer only. In the standard treatment, films were sintered at 550 °C for 15 min in an air stream. TiO<sub>2</sub> was scraped off except for a 5 mm square on a 14 mm × 16 mm slide, which served as the photoelectrode. Film thickness was measured by profilometry (Tencor Instruments alpha-step 200) at each corner of the

\* To whom correspondence should be addressed. E-mail: agrios@northwestern.edu.

† Present address: Center of Molecular Devices, Department of Chemistry, Physical Chemistry, Royal Institute of Technology (KTH), Teknikringen 30, 100 44 Stockholm, Sweden.

- (1) Decher, G. *Science* **1997**, *277*, 1232–1237.
- (2) Crisp, M. T.; Kotov, N. A. *Nano Lett.* **2003**, *3*, 173–177.
- (3) Shiratori, S. S.; Ito, T.; Yamada, T. *Colloids Surf., A* **2002**, *198–200*, 415–423.
- (4) Shiratori, S. S.; Rubner, M. F. *Macromolecules* **2000**, *33*, 4213–4219.
- (5) Shiratori, S. S.; Yamada, M. *Polym. Adv. Technol.* **2000**, *11*, 810–814.
- (6) Yoo, D.; Shiratori, S. S.; Rubner, M. F. *Macromolecules* **1998**, *31*, 4309–4318.
- (7) Lowman, G. M.; Hammond, P. T. *Small* **2005**, *1*, 1070–1073.
- (8) Dante, S.; Hou, Z.; Risbud, S.; Stroeve, P. *Langmuir* **1999**, *15*, 2176–2182.
- (9) Dutta, A. K.; Jarero, G.; Zhang, L.; Stroeve, P. *Chem. Mater.* **2000**, *12*, 176–181.
- (10) Joly, S.; Kane, R.; Radzilowski, L.; Wang, T.; Wu, A.; Cohen, R. E.; Thomas, E. L.; Rubner, M. F. *Langmuir* **2000**, *16*, 1354–1359.
- (11) Wang, T. C.; Rubner, M. F.; Cohen, R. E. *Langmuir* **2002**, *18*, 3370–3375.
- (12) Zhang, L.; Dutta, A. K.; Jarero, G.; Stroeve, P. *Langmuir* **2000**, *16*, 7095–7100.
- (13) Kovtyukhova, N.; Ollivier, P. J.; Chizhik, S.; Dubravin, A.; Buzaneva, E.; Gorchinskiy, A.; Marchenko, A.; Smirnova, N. *Thin Solid Films* **1999**, *337*, 166–170.
- (14) Kovtyukhova, N. I.; Gorchinskiy, A. D.; Waraksa, C. *Mater. Sci. Eng., B* **2000**, *69–70*, 424–430.
- (15) Cassagneau, T.; Fendler, J. H.; Mallouk, T. E. *Langmuir* **2000**, *16*, 241–246.
- (16) Cassagneau, T.; Mallouk, T. E.; Fendler, J. H. *J. Am. Chem. Soc.* **1998**, *120*, 7848–7859.
- (17) Kovtyukhova, N. I.; Martin, B. R.; Mbindyo, J. K. N.; Mallouk, T. E.; Cabassi, M.; Mayer, T. S. *Mater. Sci. Eng., C* **2002**, *19*, 255–262.

- (18) Kovtyukhova, N. I.; Martin, B. R.; Mbindyo, J. K. N.; Smith, P. A.; Razavi, B.; Mayer, T. S.; Mallouk, T. E. *J. Phys. Chem. B* **2001**, *105*, 8762–8769.
- (19) Gao, M.; Richter, B.; Kirstein, S.; Möhwald, H. *J. Phys. Chem. B* **1998**, *102*, 4096–4103.
- (20) Hu, X.; Cheng, W.; Wang, T.; Wang, Y.; Wang, E.; Dong, S. *J. Phys. Chem. B* **2005**, *109*, 19385–19389.
- (21) Hao, W.; Pan, F.; Wang, T. *J. Mater. Sci.* **2005**, *40*, 1251–1253.
- (22) Ding, B.; Kim, J.; Kimura, E.; Shiratori, S. *Nanotechnology* **2004**, *15*, 913–917.
- (23) McKenzie, K. J.; Marken, F. *Langmuir* **2003**, *19*, 4327–4331.
- (24) Milsom, E. V.; Perrott, H. R.; Peter, L. M.; Marken, F. *Langmuir* **2005**, *21*, 9482–9487.
- (25) Grätzel, M. *J. Photochem. Photobiol., C* **2003**, *4*, 145–153.
- (26) He, J.-A.; Mosurkal, R.; Samuelson, L. A.; Li, L.; Kumar, J. *Langmuir* **2003**, *19*, 2169–2174.
- (27) Wang, P.; Zakeeruddin, S. M.; Comte, P.; Charvet, R.; Humphry-Baker, R.; Grätzel, M. *J. Phys. Chem. B* **2003**, *107*, 14336–14341.

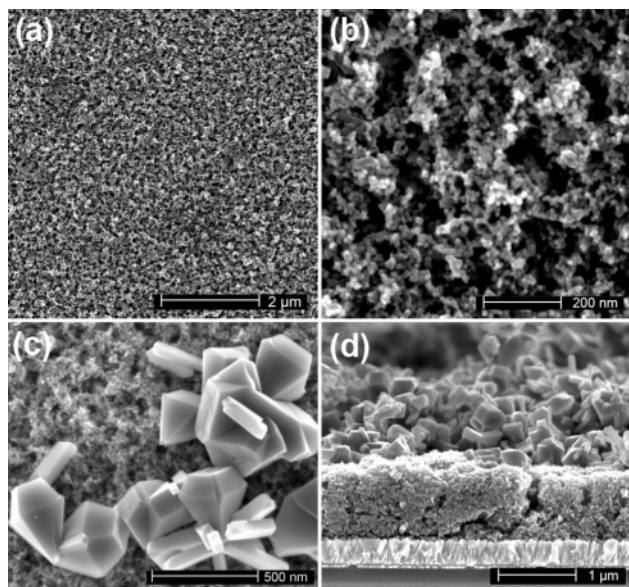


**Figure 1.** HR-SEM images of (a, b) top views of nanoparticulate films, (c) top view of scattering particles over nanoparticulate film, (d) cross-section of a nanoparticulate film topped with a scattering layer.

square, with the four results averaged to give a single value for the film. The electrode was then heated to 450 °C for 30 min, cooled to 80 °C, and immersed immediately in N719 dye<sup>28</sup> (*cis*-dithiocyanato-*N,N'*-bis(2,2'-bipyridyl-4-carboxylic acid-4'-tetrabutylammonium carboxylate) ruthenium(II), 0.5 mM in 1:1 1-butanol:acetonitrile) overnight. Counterelectrodes were 14 mm × 16 mm pieces of TEC-15 platinized with a drop of H<sub>2</sub>PtCl<sub>6</sub> and heated at 400 °C for 10 min. Dyed electrodes were rinsed in acetonitrile and sealed against a counterelectrode with 25- $\mu$ m Surlin 1702 (DuPont). Electrolyte (0.6 M BMII, 0.05 M I<sub>2</sub>, 0.5 M *tert*-butylpyridine, 0.1 M LiI in 1:1 acetonitrile:valeronitrile) was added by vacuum-release through a single hole. Cells were tested under AM 1.5 G light of 1000 W m<sup>-2</sup>.

Scanning electron microscopy of a sintered film with 5 cycles of TiO<sub>2</sub> nanoparticles shows that the particles are well-distributed and completely cover the transparent conducting oxide substrate (Figure 1a). Furthermore, mesopores, which facilitate diffusion of the electrolyte, are visible in the structure (Figure 1b). The mesopores are believed to be vacated sites that were occupied by the polymer and that may have expanded during the combustion and release of the incorporated polymer during sintering.

A typical example of a film made by coating 50 polymer-TiO<sub>2</sub> cycles on TEC-15 was 1.5  $\mu$ m thick after sintering. This represents an average of about 30 nm per cycle, or roughly 1.9 monolayers of TiO<sub>2</sub>. Made into a solar cell, it gives the full-sun current-voltage ( $J$ - $V$ ) and incident photon-to-electron conversion efficiency (IPCE) curves shown in Figure 2 (solid line) and has the performance characteristics given in Table 1. The performance is unusually good for a film of this thickness. Nanoparticulate solar cells made from films that were not sintered but instead heated to 150 °C to drive off water before dye adsorption

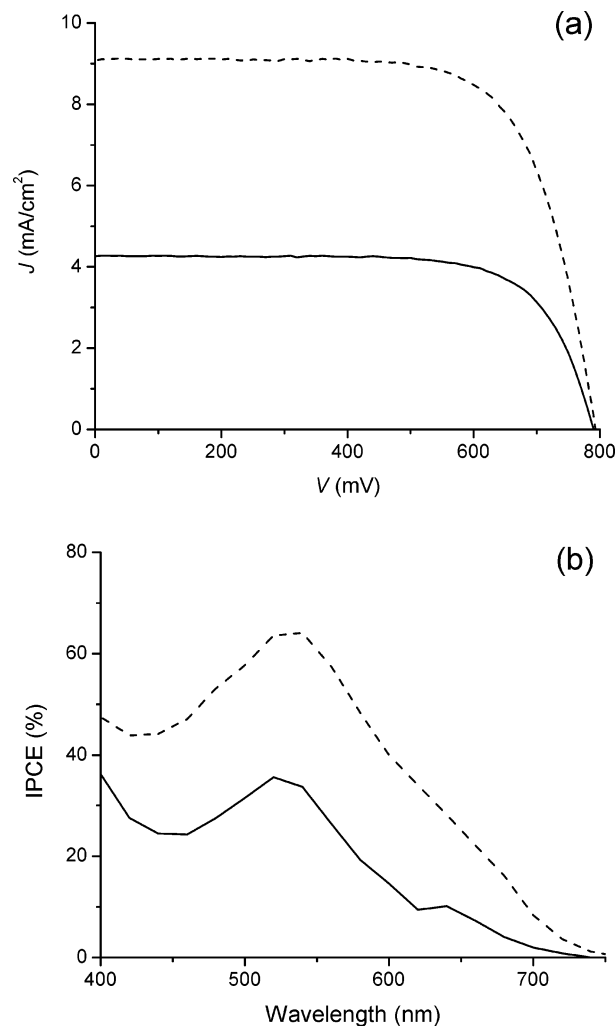


**Figure 2.** Plots showing (a) current-voltage characteristics and (b) IPCE for solar cells made from a transparent TiO<sub>2</sub> film (solid line) or a transparent film plus a scattering layer (dashed line).

**Table 1. Parameters for Solar Cells with and without Scattering Layer**

param	transparent	transparent + scattering
thickness ( $\mu$ m)	1.5	1.5 + 4.1
peak IPCE (%)	35.6	64.1
$J_{SC}$ (mA/cm <sup>2</sup> )	4.27	9.07
$V_{OC}$ (mV)	789	793
FF (%)	71.9	71.2
efficiency (%)	2.42	5.12

have the same  $V_{OC}$  and FF as films made from sintered cells; however, they have 20% lower  $J_{SC}$  and therefore 20% lower total efficiency. This raises the possibility of layer-by-layer deposition as a low-temperature fabrication method, and future work will assess its utility on flexible substrates.

Spectroscopic measurement of a dye-coated film in acetonitrile found a dye concentration within the film of 0.15 mM, based on an extinction coefficient of  $1.4 \times 10^4$  M<sup>-1</sup> cm<sup>-1</sup> at 540 nm for N719.<sup>28</sup> Given an area of 180 Å<sup>2</sup> per dye molecule,<sup>29</sup> this corresponds to a dye coverage of 210 cm<sup>2</sup> of dye per cm<sup>2</sup> of film (projected area). For a film made of 16 nm particles and assumed to have a porosity of 60%, the roughness factor is 195 cm<sup>2</sup> of surface area per cm<sup>2</sup> of

(28) Nazeeruddin, M. K.; Zakeeruddin, S. M.; Humphry-Baker, R.; Jirousek, M.; Liska, P.; Vlachopoulos, N.; Shklover, V.; Fischer, C.-H.; Grätzel, M. *Inorg. Chem.* **1999**, *38*, 6298–6305.

(29) Fillinger, A.; Parkinson, B. A. *J. Electrochem. Soc.* **1999**, *146*, 4559–4564.

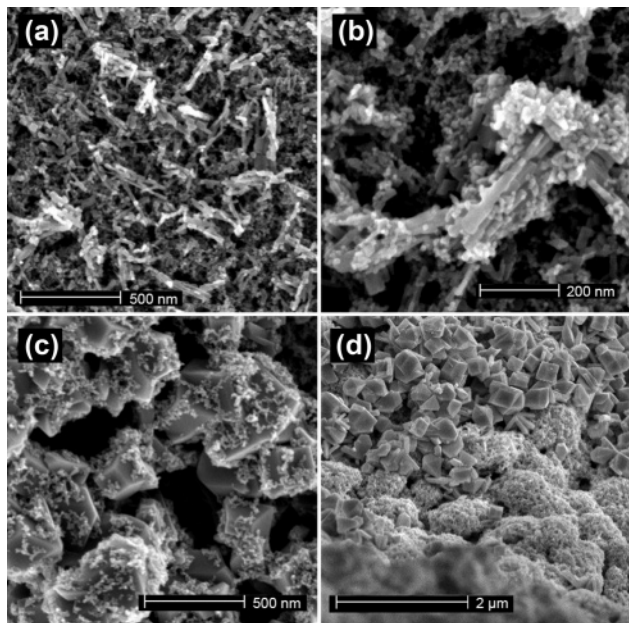


**Figure 3.** HR-SEM images of (a) a single layer of nanorods on a nanoparticulate film, (b) a single layer of nanoparticles on nanorods, (c) a single layer of nanoparticles on scattering particles, (d) a composite film showing (below) scattering particles completely coated by nanoparticles and (top) the final, uncoated layer of scattering particles.

projected area. These two numbers are in close agreement, indicating monolayer dye coverage.

A 50-cycle layer of highly scattering large-particle  $\text{TiO}_2$  (provided by CCIC, Japan) was coated on top of a 50-cycle layer of nanoparticulate  $\text{TiO}_2$ . The large particles range in size from 250 to 400 nm and are nonporous. The thickness of the scattering layer was  $4.1 \mu\text{m}$ . A solar cell made from this film is described in Figure 2a (dashed line) and Table 1 and shown in images c and d of Figure 1. The solar cell including a scattering layer had more than double the current of the transparent layer-only cell, while maintaining a similar  $V_{\text{OC}}$  and FF. The improvement in IPCE is shown in Figure 2b. A scattering layer by itself produces a current density of  $1.8 \text{ mA/cm}^2$ , accounting for 38% of the improvement due to the scattering layer over nanoparticulate  $\text{TiO}_2$ . Therefore,

the higher current in the scattering cell is primarily due to light scattered from, rather than absorbed within, the scattering layer.

Two different nanocomposite films were prepared. Neither resulted in an improvement in cell performance versus the above cells, but they illustrate the types of novel structures that are possible with the ELBL method. In one film, 5-cycle layers of nanoparticles were alternated with 1-cycle layers of  $\text{TiO}_2$  nanorods (from CCIC), with the expectation that the nanorods would penetrate the nanoparticulate layers and act as conduits for the rapid transport of electrons through the film. SEM shows that the nanorods coat very well on top of the nanoparticulate layers (Figure 3a), and vice-versa (Figure 3b).

In another film, 10-cycle layers of nanoparticles were alternated with 10-cycle layers of scattering particles in order to lengthen the optical path of photons through the nanoparticles. The deposition did not result in the intended alternating layered structure because of the size incompatibility of the different particles. However, the resulting structure proved interesting: the nanoparticles completely coat the large particles (images c and d of Figure 3). With further optimization, this could be a highly favorable structure, with large particles providing scattering and large pore volumes and coatings of small particles providing large surface area.

In conclusion, we have shown that the ELBL method can produce  $\text{TiO}_2$  films for DSCs with high efficiencies at low thickness and that this method shows promise as a low-temperature technique for fabrication on flexible substrates. Furthermore, the method opens wide possibilities for creating ordered layered films of different materials with nearly monolayer resolution, allowing for nanocomposite architectures.

**Acknowledgment.** We thank the Centre Interdisciplinaire de Microscopie Electronique for assisting in the SEM imaging. This work was supported by the U.S. National Science Foundation under Grant OISE-0402129.

CM061679U